



Direct test of static stress versus dynamic stress triggering of aftershocks

Fred F. Pollitz¹ and Malcolm J. S. Johnston¹

Received 1 May 2006; revised 12 June 2006; accepted 20 June 2006; published 11 August 2006.

[1] Aftershocks observed over time scales of minutes to months following a main shock are plausibly triggered by the static stress change imparted by the main shock, dynamic shaking effects associated with passage of seismic waves from the main shock, or a combination of the two. We design a direct test of static versus dynamic triggering of aftershocks by comparing the near-field temporal aftershock patterns generated by aseismic and impulsive events occurring in the same source area. The San Juan Bautista, California, area is ideally suited for this purpose because several events of both types of $M \sim 5$ have occurred since 1974. We find that aftershock rates observed after impulsive events are much higher than those observed after aseismic events, and this pattern persists for several weeks after the event. This suggests that, at least in the near field, dynamic triggering is the dominant cause of aftershocks, and that it generates both immediate and delayed aftershock activity. **Citation:** Pollitz, F. F., and M. J. S. Johnston (2006), Direct test of static stress versus dynamic stress triggering of aftershocks, *Geophys. Res. Lett.*, 33, L15318, doi:10.1029/2006GL026764.

1. Introduction

[2] Are aftershocks triggered primarily by the static stress change imparted by the main shock or dynamic stress changes associated with wave propagation? Many studies of well-known main shock-aftershock sequences demonstrate the importance of the static stress change for controlling the later (post-1 month) aftershock occurrence [Harris, 1998; Stein, 1999]. On the other hand, observations of aftershocks occurring during or shortly after passage of the surface waves demonstrate the strong role of dynamic triggering [e.g., Kilb *et al.*, 2000; Gomberg *et al.*, 2003; Freed, 2005]. It is also thought that delayed aftershocks in several cases are the effect of dynamic rather than static stress triggering [Parsons, 2005]. The relative importance of the two mechanisms is difficult to judge because unequivocal dynamic triggering effects, e.g., those associated with passage of the high-amplitude surface waves, are observed for only a few large main shocks. The directivity of aftershock activity [Gomberg *et al.*, 2003] and the distance dependence of aftershocks [Felzer and Brodsky, 2006] each suggest a dominance of dynamic over static stresses in triggering near-field aftershocks.

[3] A direct test of the competing hypotheses is available in the San Juan Bautista area of the San Andreas fault

(SAF), where both aseismic and seismic (impulsive) events of about the same moment release (3×10^{16} Nm), equivalent to $M \sim 5$ earthquakes, occur often (Figure 1). Since the aseismic events generate no radiated waves, examination of the aftershock patterns following aseismic and seismic events can illuminate the relative importance of the static stress change and dynamic stresses. Within a ~ 240 km² area surrounding a 30 km-long part of the SAF near San Juan Bautista, both aseismic and seismic events of comparable magnitude (near M_5) have occurred, and the local seismicity catalog is complete to $M = 1.5$ since 1974. We characterize the aftershock sequences of both classes of events using an Omori law. Comparison between the two classes shows that aftershock rates following seismic events are much larger than those following similar aseismic events. This strongly suggests that, at least in the near field, dynamic stresses are the dominant cause of aftershocks for several weeks following a main shock.

2. Observed Aftershock Sequences

[4] We select five seismic and four aseismic events of $M \sim 5$ that occurred in the San Juan Bautista region from 1974 to 2004 (Figure 1). (All events of magnitude ≥ 4.5 during this time period, excluding Loma Prieta aftershocks, are included.) Magnitudes and locations of seismic events are from the Northern California Earthquake Data Center. For the aseismic events this information is based on strainmeter recordings, and it is further guided by the locations of small earthquakes that accompany the relatively large aseismic slip events or sub-events [Linde *et al.*, 1996; Johnston and Linde, 2002]. The (equivalent magnitude) $M \sim 4.9$ 19 April 1996 aseismic slip event was preceded by a $M = 4.7$ impulsive slip event, and the total moment associated with aseismic slip was about 2.5 times that of the seismic slip [Johnston *et al.*, 1996]. Thus we classify the composite event as aseismic. The $M = 5.1$ 12 August 1998 impulsive event [Uhrhammer *et al.*, 1999] was followed by aseismic slip lasting two to three weeks [Gwyther *et al.*, 2000]. Based on the coseismic and postseismic strain changes at local borehole tensor strainmeter SJT and aftershock locations, Gwyther *et al.* [2000] infer an equivalent moment $M_5.0$ of the aseismic slip compared with 5.2 of the coseismic slip. The lower aseismic moment is consistent with our classification of the composite event as an impulsive event. The $M \sim 5$ aseismic slip event of 16 March 2004 is associated with a magnitude 4.3 earthquake, and we classify the composite event as aseismic. A few other impulsive events of magnitude 4.5 occurred during the time period considered, but their interpretation is complicated by the occurrence of two or more $M 4$ events within several days of each other. Like the impulsive events included here, these composite events are associated with vigorous aftershock

¹U.S. Geological Survey, Menlo Park, California, USA.

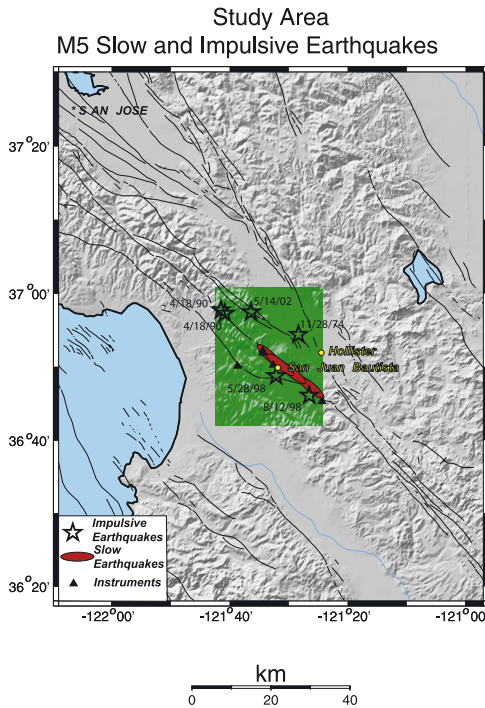


Figure 1. Seismicity of the San Juan Bautista, California, area from 1974 to 2004. Green rectangular area indicates the study area. Large stars indicate the epicenters of $M \sim 5$ impulsive events, and ovals indicate the rupture areas of $M \sim 5$ aseismic events. Triangles are the locations of strainmeters used to localize the aseismic events.

activity but are more difficult to model with a simple aftershock-decay law.

[5] Based on strainmeter recordings, the aseismic events generally have a total duration of several days, but most of the moment release associated with them is completed within 0.25 to 2 days [Linde *et al.*, 1996; Johnston and Linde, 2002]. The “origin time” of a typical aseismic event is thus ambiguous on this timescale. We associate a single origin time with each aseismic event chosen at a time where about 80% of the associated strain offsets have been completed. Aftershocks are counted strictly starting at the origin time. Although “aftershocks” begin accumulating at the initiation of each aseismic event, our conclusions would be unaffected by choosing an origin time at the initiation, rather than the effective termination, of each aseismic event.

[6] Cumulative seismicity of $M \geq 1.5$ spanning the times of these impulsive and aseismic events (main shocks) are shown in Figure 2. Both sets of events are followed by aftershocks at rates that exceed pre-event seismicity rates. However, visual comparison between the sets of impulsive and aseismic events reveals that aftershock activity is more vigorous after the impulsive events than the aseismic events. This pattern is remarkable given that the corresponding source areas have been roughly equally productive in generating earthquakes over a wide range of magnitudes (Figure S1a in the auxiliary material).¹ This is explored in greater detail in Table S1 by considering both average and

background seismicity rates in selected subregions over the 31-year period. Using either measure of seismicity rates, the source area of the large aseismic events is at least as productive as the source areas of the largest impulsive events, demonstrating that the former is equally capable of generating smaller events and hence aftershocks. The comparable seismic activity in slow- and impulsive-earthquake generating areas is verified in depth cross-sections (Figures S1b and S1c). This suggests that differences in aftershock rates are not substantially biased by either the locations of the main shocks, systematic differences in the locations of the aftershocks, or fundamental differences in the properties of the source areas. Finally, source areas of the slow events appear to occur on patches creeping at about one-third of the long-term slip rate [Johanson and Bürgmann, 2005], supporting the notion that the same source areas are capable of generating both impulsive and aseismic events.

3. Quantification With Omori’s Law

[7] A modified form of Omori’s law [Utsu, 1961] describes the decay rate of seismic activity after a main shock as

$$r(t, m) = \frac{dN}{dt} = \frac{1}{\tau} \left[1 + \frac{t}{c(m)} \right]^{-p} \quad (1)$$

where $r(t, m)$ is the rate of aftershocks of magnitude greater than m at time t after the main shock, $c(m)$ is a magnitude-dependent constant and τ and p are constants. One may integrate equation (1) with respect to time to obtain the cumulative number of aftershocks of magnitude greater than m :

$$N(t, m) = \int_0^t r(t', m) dt' = \begin{cases} \frac{1}{\tau p - 1} \left\{ 1 - \left[1 + \frac{t}{c(m)} \right]^{1-p} \right\} & p \neq 1 \\ \frac{1}{\tau} c(m) \log \left(1 + \frac{t}{c(m)} \right) & p = 1 \end{cases} \quad (2)$$

The lower magnitude threshold is fixed at $m = 1.5$, above which the seismicity catalog is considered complete.

[8] One may characterize every aftershock sequence with a set of constants $\{\tau, c, p\}$. In order to make comparison between impulsive and slow events as direct as possible, it is preferable to find a combination $\{c, p\}$ that is applicable to every event; differences between events would then be represented by differences in inferred τ . The strategy for modeling the observed aftershock sequences (Figure 2) consists of the following steps:

[9] 1. For every event independently, estimate the pre-event seismicity rate and correct the cumulative-seismicity data for this rate. This step was applied prior to plotting the cumulative seismicity rates in Figure 2 using 110 days of background seismicity. The average pre-event (background) seismicity rates are consistently in the range 0.2 to 0.25 $m \geq 1.5$ events/day prior to each source earthquake.

[10] 2. Perform a grid search over c and p . For each pair $\{c, p\}$, τ is determined for every event using a least squares inversion of observed $N(t, m)$ fitted to the function given in equation (2). The first 40 days of aftershocks are used in this

¹Auxiliary material data sets are available at <ftp://ftp.agu.org/apend/gl/2006gl026764>. Other auxiliary material files are in the HTML.

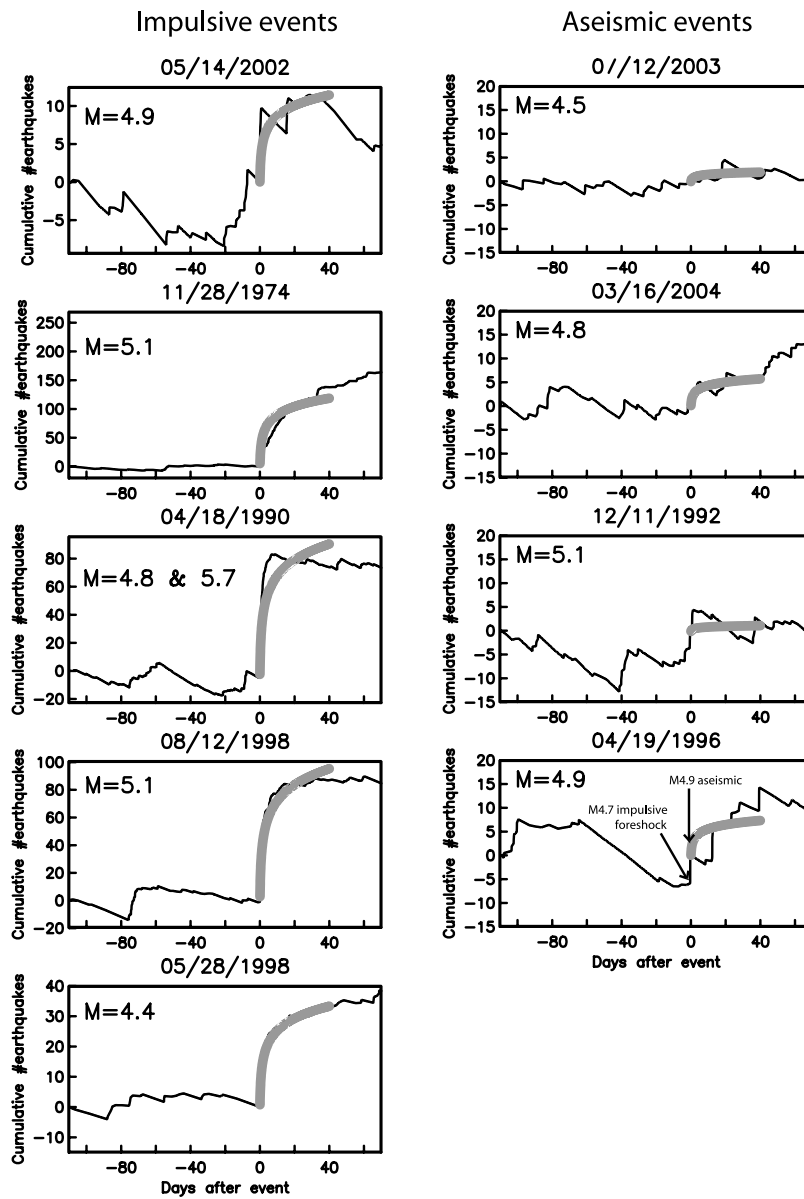


Figure 2. Black curves: Cumulative number of seismic events of magnitude ≥ 1.5 around the times of selected (a) impulsive events and (b) aseismic events. The curves have been corrected for pre-event seismicity rates using 110 days of regional seismicity prior to each event. Thick gray curves show the corresponding fit to the cumulative seismicity after optimal fitting for optimal Omori's law parameters, using the functional form of equation (2).

step. The values of c and p which yield a global minimum misfit (over all impulsive and aseismic events summed up) are taken as the optimal c and p .

[11] 3. The inverse decay rate τ may then be estimated for every event with the above-determined values of c and p .

[12] Application of this procedure to the cumulative-seismicity data of Figure 2 results in optimal values of the constants $c = 0.15$ day and $p = 1.01$. The associated aftershock rates τ^{-1} estimated for each event are shown in Figure 3. A clear pattern emerges from the quantitative fits, impulsive events being associated with much larger τ^{-1} than aseismic events. Put another way, the aftershock rates of impulsive events are a factor of about two to twenty larger than those of similar-sized aseismic events. Although aftershock duration for the various impulsive events is

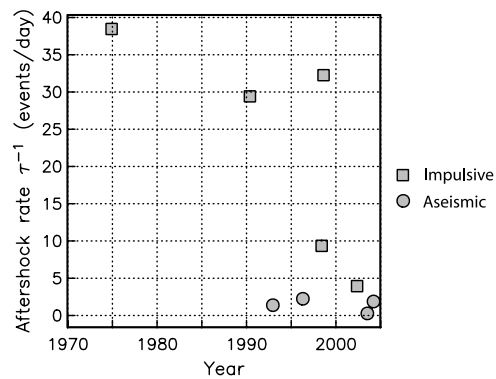


Figure 3. Seismicity rates τ^{-1} derived from the observed cumulative aftershock distributions $N(t, m)$ (Figure 2), grouped into impulsive and aseismic events.

variable (ranging from 10 to 60 days) and aseismic events are poorly fit by the modified Omori law, other measures of aftershock rate yield the same conclusion (Figure S2).

4. Discussion

[13] Postseismic stress triggering associated with viscoelastic relaxation of the lower crust or mantle, which has been advanced as an important mechanism following $M \gtrsim 7$ main shocks [Pollitz and Sacks, 1997; Freed and Lin, 2001; Pollitz and Sacks, 2002], is unlikely to play a role in generating the observed aftershocks in this study because of the relatively low magnitudes of the main shocks in the San Juan Bautista source area. In addition this mechanism would be expected to act equally for similar-sized impulsive and aseismic main shocks and therefore could not explain the difference in temporal aftershock patterns.

[14] Another mechanism affecting aftershock rates would be the response of seismicity to a stress step governed by rate and state friction [Dieterich, 1994]. Since aftershock rates are highest during the first few days after an event, an aseismic event (which takes place over a timescale of several hours to about 1 day) might be expected to generate fewer aftershocks after “completion” of the event. We investigate this quantitatively by employing equation (B14) of Dieterich [1994] for the evolution of the state variable γ subject to a shear stress step with values of background stressing rate $\dot{\tau}_r$, prescribed background seismicity rate r , and initial value of the state variable $\gamma = 1/\dot{\tau}_r$. A slow-slip event is realized as a superposition of small slip events distributed uniformly over a time Δt , associated with a net stress step $\Delta\tau$ on a surrounding fault. We integrate equation (B14) of Dieterich [1994] with respect to time for a linear stress dependence with slope $\Delta\tau/\Delta t$ to obtain γ after termination of the slow event, then continue integration of equation (B14) using the post-event stressing rate $\dot{\tau}$, which is assumed to be constant. Substituting the resulting γ into equation (11) of Dieterich [1994] yields

$$\dot{N} = \frac{r\dot{\tau}/\dot{\tau}_r}{\left\{ \left[\frac{\dot{\tau}}{\dot{\tau}_r} - \beta \right] \exp\left(-\frac{\Delta\tau}{A\sigma}\right) + \beta - 1 \right\} \exp(-t/t_a) + 1} \quad (3)$$

$$\beta = \frac{\Delta\tau}{\Delta\tau} \dot{\tau} \quad (4)$$

where aftershock duration t_a is given by equation (14) of Dieterich [1994] and the product $A\sigma$ is assumed constant and, for a given t_a , is prescribed by the same equation. Time t is measured following termination of the slow-slip event. We choose the value $t_a = 25$ days, assume $\dot{\tau} = \dot{\tau}_r$, and explore a range of values of $\Delta\tau$ from 1 to 30 bars and $\dot{\tau}_r = 0.1$ to 0.2 bars/yr, which are typical stressing rates for the plate boundary zone. Cumulative seismicity N [impulsive] and N [aseismic] are generated as a function of time and their ratio evaluated for values of Δt ranging from 0.5 to 3 days. Results are not very sensitive to choices of $\Delta\tau$ and $\dot{\tau}_r$ in the ranges indicated above. Figure S3 shows the predicted ratio versus time for $\Delta\tau = 1$ bar and $\dot{\tau}_r = 0.2$ bars/yr; these parameter values are at the ends of the considered ranges to produce the smallest ratios. Within a short time after an

event, cumulative number of aftershocks following aseismic events are generally $\geq 90\%$ of that following impulsive events. Given the much larger disparity in observed aftershock production rates following the two classes of events (Figure 3), different responses to a shear stress step are unlikely to be the explanation.

[15] We suggest the underlying cause of this phenomenon to be a change in the state of faults surrounding the main shock upon passage of the seismic waves. This may be realized by a reduction in the net area of contact surfaces across these faults [e.g., Parsons, 2005]. This is consistent with the increase in acoustic emissions witnessed in pre-faulted rock samples subject to a cyclical stress step [Lavrov, 2005]. If true, then application of rate and state friction theory to aftershocks would involve a dichotomy between impulsive and aseismic events. One must account for two effects for an impulsive rupture, i.e., both a stress step and a dynamically-induced change in state of surrounding faults, but for a slow rupture only a stress step (distributed over the duration of the slow rupture) enters into consideration.

[16] The dominance of dynamic stress effects in generating aftershocks for several weeks apparently contradicts solid evidence for static stress triggering. The latter is best demonstrated by the spatial correlation between areas of elevated change in Coulomb failure stress and aftershocks [Harris, 1998; Stein, 1999]. Detailed consideration of the temporal dependence of aftershock activity following the 1999 Chi Chi earthquake, however, led Ma *et al.* [2005] to conclude that dynamic stress triggering was dominant for a period of three months, after which static stress triggering emerged as the dominant mechanism. Despite the relatively small impact of the static stress change in the short term, its importance remains tangible. Three of the four aseismic events considered here have aftershock rates τ^{-1} of 1.4 to 2.2 events/day, well above the background rate of ~ 0.2 events/day. In addition, the large aseismic slip event of 16 March 2004 and a small aseismic slip event on 12 August 1998 were followed within hours by magnitude 4.3 and 5.1 earthquakes, respectively, probably because of the static stress change imparted by the aseismic events.

5. Conclusions

[17] Aftershock rates for several weeks following impulsive events (i.e., earthquakes) in the San Juan Bautista area are much higher than those following aseismic events of similar magnitude. The “main shocks” occupy similar source areas, and the aftershock areas similarly overlap, so that differences in the temporal decay pattern do not appear to be related to any difference in source region. These results apply to a ~ 240 km² area surrounding the SAF. They imply that the dominant mechanism of near-field aftershock triggering is dynamic stresses and that this mechanism not only acts instantaneously (upon passage of the seismic waves from the main shock) but also generates continued aftershock activity with a delay of up to several weeks.

[18] **Acknowledgments.** This paper benefitted from the constructive comments of two anonymous reviewers. We thank Roland Bürgmann, Ingrid Johanson, Tom Parsons, Bob Simpson, Ross Stein, and Wayne Thatcher for their comments on a preliminary draft.

References

- Dieterich, J. (1994), A constitutive law for earthquake production and its application to earthquake clustering, *J. Geophys. Res.*, *99*, 2601–2618.
- Felzer, K. R., and E. E. Brodsky (2006), Decay of aftershock density with distance indicates triggering by dynamic stress, *Nature*, *441*, 735–738.
- Freed, A. (2005), Earthquake triggering by static, dynamic, and postseismic stress transfer, *Annu. Rev. Earth Planet. Sci.*, *33*, 335–368.
- Freed, A., and J. Lin (2001), Delayed triggering of the 1999 Hector Mine earthquake by viscoelastic stress transfer, *Nature*, *411*, 180–183.
- Gomberg, J. S., P. Bodin, and P. A. Reasenberg (2003), Observing earthquakes triggered in the near field by dynamic deformations, *Bull. Seismol. Soc. Am.*, *93*, 118–138.
- Gwyther, R. L., C. H. Thurber, M. T. Gladwin, and M. Mee (2000), Seismic and aseismic observations of the 12th August 1998 San Juan Bautista, California M_w 5.3 earthquake, paper presented at 3rd San Andreas Fault Conference, Stanford Univ., Stanford, Calif.
- Harris, R. (1998), Introduction to special section: Stress triggers, stress shadows, and implications for seismic hazard, *J. Geophys. Res.*, *103*, 24,347–24,358.
- Kilb, D., J. S. Gomberg, and P. Bodin (2000), Triggering of earthquake aftershocks by dynamic stresses, *Nature*, *408*, 570–574.
- Johanson, I. A., and R. Bürgmann (2005), Creep and quakes on the northern transition zone of the San Andreas fault from GPS and InSAR data, *Geophys. Res. Lett.*, *32*, L14306, doi:10.1029/2005GL023150.
- Johnston, M. J. S., and A. T. Linde (2002), Implications of crustal strain during conventional, slow, and silent earthquakes, in *International Handbook of Earthquake and Engineering Seismology, Int. Geophys. Ser.*, vol. 81A, pp. 589–605, Elsevier, New York.
- Johnston, M. J. S., R. Gwyther, A. T. Linde, M. Gladwin, G. D. Myren, and R. J. Mueller (1996), Another slow earthquake on the San Andreas fault triggered by a $M4.7$ earthquake on April 19, 1996, *Eos Trans. AGU*, *77*, 515.
- Lavrov, A. (2005), Fracture-induced physical phenomena and memory effects in rocks: A review, *Strain*, *41*, 135–149.
- Linde, A. T., M. T. Gladwin, M. J. S. Johnston, R. L. Gwyther, and R. Bilham (1996), A slow earthquake near San Juan Bautista, California, in December, 1992, *Nature*, *383*, 65–68.
- Ma, K. F., C. H. Chan, and R. S. Stein (2005), Response of seismicity to Coulomb stress triggers and shadows of the 1999 $M_w = 7.6$ Chi-Chi, Taiwan, earthquake, *J. Geophys. Res.*, *110*, B05S19, doi:10.1029/2004JB003389.
- Mueller, R. J., and M. J. S. Johnston (2000), Deformation along the San Andreas fault south of the coseismic and postseismic October 18, 1989, Loma Prieta M_L 7.1 earthquake rupture, *U.S. Geol. Surv. Open File Rep.*, *00-146*.
- Parsons, T. (2005), A hypothesis for delayed dynamic earthquake triggering, *Geophys. Res. Lett.*, *32*, L04302, doi:10.1029/2004GL021811.
- Pollitz, F. F., and I. S. Sacks (1997), The 1995 Kobe, Japan, earthquake: A long-delayed aftershock of the offshore 1944 Tonankai and 1946 Nankaido earthquakes, *Bull. Seismol. Soc. Am.*, *87*, 1–10.
- Pollitz, F. F., and I. S. Sacks (2002), Stress triggering of the 1999 Hector Mine earthquake by transient deformation following the 1992 Landers earthquake, *Bull. Seismol. Soc. Am.*, *92*, 1487–1496.
- Stein, R. S. (1999), The role of stress transfer in earthquake occurrence, *Nature*, *402*, 605–609.
- Uhrhammer, R., L. S. Gee, M. Murray, D. Dreger, and B. Romanowicz (1999), The M_w 5.1 San Juan Bautista, California earthquake of 12 August 1998, *Seismol. Res. Lett.*, *70*, 10–18.
- Utsu, T. (1961), A statistical study on the occurrence of aftershocks, *Geophys. Mag.*, *30*, 521–605.

M. J. S. Johnston and F. F. Pollitz, U.S. Geological Survey, 345 Middlefield Road, MS 977, Menlo Park, CA 94025, USA. (fpollitz@usgs.gov)